

# RSC Advances



This is an *Accepted Manuscript*, which has been through the Royal Society of Chemistry peer review process and has been accepted for publication.

*Accepted Manuscripts* are published online shortly after acceptance, before technical editing, formatting and proof reading. Using this free service, authors can make their results available to the community, in citable form, before we publish the edited article. This *Accepted Manuscript* will be replaced by the edited, formatted and paginated article as soon as this is available.

You can find more information about *Accepted Manuscripts* in the [Information for Authors](#).

Please note that technical editing may introduce minor changes to the text and/or graphics, which may alter content. The journal's standard [Terms & Conditions](#) and the [Ethical guidelines](#) still apply. In no event shall the Royal Society of Chemistry be held responsible for any errors or omissions in this *Accepted Manuscript* or any consequences arising from the use of any information it contains.

## REVIEW ARTICLE

# Overview on *in vitro* and *in vivo* investigations of nanocomposite based cancer diagnosis and therapeutics

Cite this: DOI: 10.1039/x0xx00000x

Received 00th January 2015,  
Accepted 00th January 2015

DOI: 10.1039/x0xx00000x

www.rsc.org/

A.P Subramanian<sup>a</sup>, S. K. Jaganathan<sup>\*a</sup>, Eko Supriyanto<sup>a</sup>

Cancer is the second leading cause of mortality around the globe, despite the various advancements in science. The success of the cancer treatment lies within early diagnosis and effective therapy making them inseparable. In recent years, there has been an extraordinary development in the field of nanomedicine with the development of new nanoparticles for the diagnosis and treatment of cancer. These researches are generally focused on creating novel nanocomposites for combating cancer. This review will serve as a one-stop arrangement for collating and providing future perspectives about the various nanocomposites based *in vitro* and *in vivo* investigations for cancer diagnosis and treatment. From our study, it is revealed that nanocomposite based diagnosis engrosses nanosensors for detection and conjugation of biomarkers, quantum dots, radiolabeling, delivery of contrast agent for better imaging of cancer development. In cancer therapeutics, nanocomposites hold enormous potential in maximizing the benefits of both targeted chemotherapy and photodynamic therapy. This review will encourage the need of in-depth molecular level examination in relation to the cytotoxicity and bio-distribution of the developed nanocomposite should be evaluated in the clinical setting for better understanding. These supplementary researches on nanoncology would help in personalizing cancer theranostics making nanooncology as the future trend.

## 1. Introduction

Nanomedicine is the current field of technological innovation, which embraces the use of nanomaterial and nanoelectronic biosensors. The application of nanomedicine in cancer involves both diagnosis and therapy [1]. Technology refers to the collection of techniques, which once seen as implausible to ordinary chores. The continuous thirst of scientists and engineers to various quests has spawned a new form of technology named nanotechnology [2]. Nanotechnology is the study and application of extremely small things in nanometer ( $10^{-9}$ ) and can be used across all the other scientific fields, such as chemistry, molecular biology, semiconductor physics, materials science, surface sciences and microfabrication [3].

Cancer claims to be the second cause of death worldwide. The cancer ultimately results from uncontrollable growth of cells that may spread to other parts of the body. According to the World Health Organization (WHO), about 1,658,370 new cancer cases are expected to be diagnosed in 2015 [4]. Physicians around the globe strongly believe that early detection of cancer can greatly improve the odds of successful treatment and survival. Detection of cancer is not only limited planning of treatment procedures. Various visualization techniques are used to follow the course of cancer

treatment, to monitor the metastasis formation and proper remission of the developed cancer [5]. Thus, visualization and therapeutics of cancer seem to have an interrelationship among one another for an extended instance and seems inseparable. This paper links the recently developed nano-based diagnosis and treatment methods to the killer disease cancer.

Imaging modalities like X-rays, CT, MRI and PET wisely utilizes a range of contrast agents for better diagnosis [6]. Biocompatible nanodevices made of biomaterials usually deliver these agents. This adaptation allows very high resolution and an accurate mapping of lesions facilitating the surgeons for planning the surgical removal of the tumor. More advanced nanodevices have features to detect, evaluate, treat and report to the clinical doctor automatically [7]. Cancer treatments are generally categorized as surgery, radiotherapy, chemotherapy, immunotherapy, hormone therapy, or gene therapy. Of these the chemotherapy and radiotherapy are conventional. The chemotherapists and radiotherapists still face the biggest challenge of side effects after the treatment. These conventional cancer therapies have side effects such as nausea, insomnia, delirium, vomiting, fatigue and severe hair loss. To overcome these shortcomings, several researchers and scientists focus on nanotherapeutics [8]. This nanotherapeutics mainly deals

with the targeted drug delivery by the nanocarriers, which are mostly made of nanocomposites.

Nanocomposite is a multiphase solid material where one of the phases is in nano-scale that is recently used for this purpose. Due to their quantum-scale sizes, they exhibit different properties from that of conventional microcomposites [9]. They have good biocompatibility and biodegradability apart from being thermodynamically stable within biological systems [10]. The nanocomposites are tailored, based upon the specific application. The nanodevices are synthesized using nanocomposites by the researchers around the globe. Most of their applications are related to *in vivo* visualization and therapy with anticancer drugs [11] in the field of oncology. This review emphasis only on the various *in vivo* and *in vitro* investigations of nanocomposite materials in diagnosis and therapy employed for various cancers thereby promoting them in the clinical usage (figure 1).

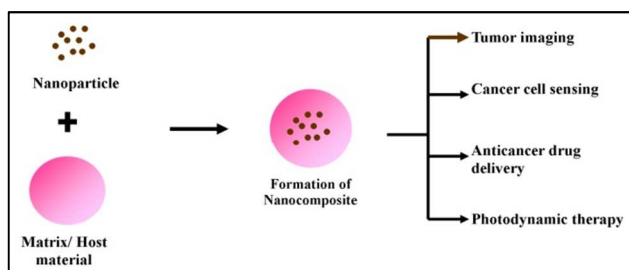


**Figure 1:** Scheme of nanocomposites and its cancer application

## 2. Nanotechnology in cancer diagnosis

Cancer diagnosis is a major phenomenon in the field of oncology as physicians believe early detection of cancer may help in long time survival of the patients. The conventional way of cancer diagnosis involves blood tests, computed tomographical imaging, magnetic resonance imaging as well as biopsy [12]. Recently the emerging trend is based on the nano-based *in vivo* visualization of various cancers. The nanodevices may contain contrast agents to enhance the ultrasound images and MRI. Some nanodevices contain quantum dots, nanoparticles with quantum confinement properties in precise imaging of tumors. Apart from these, there are nanosensors such as magnetic nanodevices conjugated with labeling molecules as well as immunosensors with cancer biomarkers that act as aptamers [13]. The various nanocomposite based systems for detection of cancer are discussed in detail.

### 2.1 *In vitro* investigations of nanocomposites based cancer diagnosis

Early nanocomposites based *in vitro* investigations involve the enhancement of imaging techniques and voltammetric analysis to improve the detection. Scientists also utilized specific peptide molecule present in the cancer cells for identification. Recent researches are mostly carried out based on the detection of specific biomarkers present in the cancer cells. Basically, a biomarker is a measurable substance in an organism whose presence is indicative of some phenomenon such as disease or infection. The nanocomposites containing these biomarkers especially antibodies/ antigens are generally termed as immunosensors. The principle involved in cancer diagnosis in

*in vitro* condition is shown diagrammatically in figure 2. Various experimentations of nanocomposite based diagnosis are further discussed.

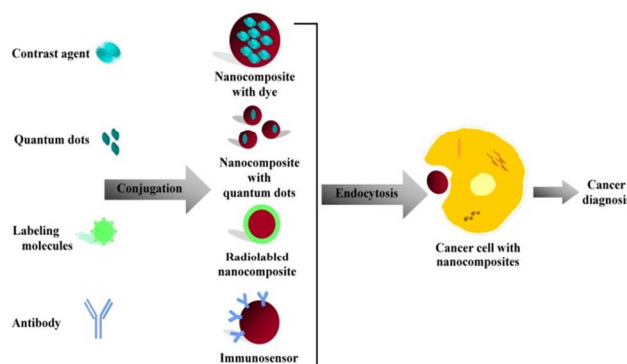


**Figure 2:** Principle involved in nanocomposite based *in vitro* visualization

Martirosyan *et al* produced a nanocomposite made of poly (methyl methacrylate) with single walled carbon nanotube to promote the interstitial brachytherapy, a treatment for prostate cancer. The treatment is usually monitored by magnetic resonance imaging. The developed nanocomposite was designed to promote the monitoring. The contrast agents (choline derivate - and gadolinium - based) are introduced inside the nanocomposite using high pressure stainless steel syringe. The polyglycolic acid was used as a biodegradable encapsulation. The *in vitro* testing of the nanocomposites showed visualization under 1.5 T, revealing the biocompatibility and radiation resistance [14].

A novel nanocomposite gel was made of gold nanoparticle and chitosen gel coated glassy carbon electrode (GCE) for immobilization and electrochemical study of K562 leukemia cells. This cell-based sensor was based on the measurement of electron-transfer resistance with  $[\text{Fe}(\text{CN})_6]^{3-/4-}$  as a redox probe. Higher amount of K562 cells was immobilized to the electrode with the increasing concentration of cells to the immersed GCE. The density of the cells adhered to the film increased with respect to the incubation time, which was evidenced by the morphology of the distinguishable filopodia, a good indicator of cell adhesion to material surfaces and cell viability [15]. A nanocomposite platform for detection of chronic myelogenous leukemia (CML) was prepared and analyzed in clinical samples. The nanocomposite was developed by deposition of nanostructured composite of Chitosan (CS)-cadmium-telluride quantum dots (CdTe-QDs) onto indium-tin-oxide coated glass substrate. After which the amine terminated probe DNA has been covalently immobilized onto CS-CdTe/ITO electrode using glutaraldehyde as a cross linker. Four cDNA samples were used to test the specificity of pDNA/CS-CdTe/ITO bioelectrode. The change in the peak current during the voltametric analysis revealed that the fabricated nucleic acid sensor had excellent scope for detection of CML in clinical patient samples [16].

Shen *et al* developed an electrochemical biosensing system for detecting leukemia cells based on  $\text{TiO}_2/\text{CNT}$  nanocomposites modified electrodes. Titanium isopropoxide and multiwalled CNT were dispersed in a ratio of 70: 30 (w/w) to form the nanocomposite. Electrochemical studies were carried out to test the ability of the developed nanocomposite with respect to detection. The peak current obtained was 10-fold higher than that without the cancer cells. The electrochemical response of the probe on the K562 cells

film is apparently stronger than that in the K562 cells film, accompanying with a 30 mV negative shift of the peak potential [17]. A novel impedance cell sensor based on the polystyrene/polyaniline/gold nanocomposite was prepared for the detection of HL-60 leukemia cells. The nanocomposite was prepared by assembling the gold nanoparticles on the surface of polystyrene (PS) and polyaniline (PANI) core-shell nanocomposite. The electrochemical sensor was suspended in the HL-60 leukemia cells for 2h. The immobilized cells exhibited irreversible voltammetric response and increased the electron transfer resistance with a good correlation to the logarithmic value of concentration ranging from  $1.6 \times 10^3$  to  $1.6 \times 10^8$  cells  $\text{mL}^{-1}$  with a limit of detection of  $7.3 \times 10^2$  cells  $\text{mL}^{-1}$  at  $10\sigma$  [18].

Bai *et al* developed a copper monosulfide nanoparticle-decorated reduced graphene oxide-based electrochemical biosensor for the reliable detection of  $\text{H}_2\text{O}_2$ . The high levels of  $\text{H}_2\text{O}_2$  are closely associated with cancer and progressive neurodegenerative diseases. The levels of extracellular  $\text{H}_2\text{O}_2$  were detected from the HeLa cell culture. This method was used to detect the  $\text{H}_2\text{O}_2$  in the human cervical cancer cell lines HeLa in phosphate-buffered saline (pH 7.4) containing 25 mM glucose at the applied potential of  $-0.27$  V versus Ag/AgCl. An increased cathodic current was observed after treatment of the HeLa cells with 0.4 mg/mL CdTe QDs. Thus, promoting CuS nanoparticle-decorated reduced graphene oxide-based electrochemical biosensor for cervical cancer detection [19].

An aptamer biosensor for breast cancer cell detection was developed on the ultrasensitive electrochemical basis. This aptamer is a probe that can recognize and bind to the MCF-7 cells. The aptamer was made up of porous graphine oxide/ Au composites and porous polytetrafluoroethylene alloy. The mucin protein 1 was selected as the tumor marker for MCF-7 breast cancer cell detection. The aptamer had an analytical performance ranging from 100 to  $5.0 \times 10^7$  cells  $\text{mL}^{-1}$  with a limitation of  $\text{mL}^{-1}$ , which was reproducible [20]. An integrated nanocomposite loaded with 5 nm gold nanoparticle conjugated with poly[9,9-bis(6'-N,N,N-trimethylammonium)hexyl)fluorenyldivinylene-alt -4,7-(2,1,3-benzothiadiazole) dibromide] (PFVBT) polymer was used for dual-modal targeted cellular imaging of MCF-7 cells. The PLGA-PEG 2000-folate was used for encapsulation of the nanocomposite. The eccentrically loaded gold nano particle helped to maintain the fluorescence. The cellular uptake of the nanocomposite was improved due to the presence of folic acid groups. The nanocomposites were then suspended in both 3T3 fibroblast cells as well as the MCF-7 breast cancer cells. The fluorescence intensities from 3T3 cells upon treatment with folic acid functionalized nanocomposites were not significantly higher than the intensities from MCF-7 cells. This was related to the presence of folic acid receptors in the cancer cells [21].

A label-free electrochemical bioanalyte immunosensor was developed for simultaneous detection of lung cancer biomarkers such as anti-MAGE A2 and anti-MAGE A11. These antibodies belong to the Melanoma Associated Gene (MAGE) that recognizes the MAGE antigens responsible for tumor progression present in the cancer cells. This was done using carbon nanotubes-chitosan (CNT-CHI) composite. They used single walled CNT and the electrodes were fabricated by drop casting method onto graphite surface. The differential pulse voltammeter (DPV) measurements displayed that both (MAGE A2/CNT-CHI/graphite and MAGE A11/CNT-CHI/graphite) immunoelectrodes had successful detection of analytes anti-MAGE A2 and anti-MAGE A11 from 5 fg  $\text{mL}^{-1}$  to 50 ng  $\text{mL}^{-1}$ . These CNT-graphite electrodes were independently

able to distinguish the anti-MAGE A2 and anti-MAGE A11 independently in a single experimental run, when exposed to a mixture of various analyte concentrations in different combinations irrespective of the presence of other analyte present in the same vessel [22]. Zhuo *et al*, developed a more susceptible method for detection of progastrin releasing-peptide (ProGRP) tumor marker with small cell lung cancer (SCLC), which may indicate an early tendency of cancer metastasis. Pro-GRP is a member of the bombesin family of peptides is produced by the SCLC cells to have mitogenic activity. The Au/TiO<sub>2</sub> nanocomposites (nano-Au/TiO<sub>2</sub>) was prepared by attaching the Au nanoparticles to the TiO<sub>2</sub> nanoparticles using the linkage reagent 3-aminopropyltriethoxysilane. After this, the glucose oxidase (GOD) and ferrocene labeled secondary antibodies (Fc-Ab2) were used to bind Au/TiO<sub>2</sub> nanocomposites to provide amplified signals. Apart from this, the nano-Au functionalized graphene sheets (GS) were used as biosensor platform to increase the surface area and the electronic transmission rate to capture a large amount of primary antibodies (Ab1). The clinical analysis was done in eleven serum samples from lung cancer patients and healthy volunteers, in order to evaluate their performance. It was found that for the proposed immunosensor, the current is linear with the concentration of ProGRP being within a concentration range from 10.0 to 500 pg/mL with a limit of detection down to 3.0 pg/mL (S/N = 3) [23].

A combined magnetic enrichment and optical detection strategy for lung cancer cells detection was developed by Ma *et al*. The bifunctional nanocomposites (BNPs) with quantum dots had excellent fluorescence with ability to conjugate with monoclonal anti-CEA antibodies, which allows specific reorganization of SPCA-1 human lung adenocarcinoma cells in short time. This antibody helps in the identification of the carcinoembryonic (CEA) antigen present in certain types of cancer cells. The BNPs was developed by modification of silica coated superparamagnetic nanoparticle (SiO<sub>2</sub>/ $\gamma$ -Fe<sub>2</sub>O<sub>3</sub>) with N-(2-aminoethyl)-3-aminopropyltrimethoxysilane and conjugated with anti-CEA antibodies. The benign and malignant pleural effusions of 10 patients was used to examine the ability of the BPNs in relation to detection. The immunonanoparticles had 70 % sensitivity and 100% specificity in the pleural effusion samples when examined within 1 hour [24]. Zhao *et al* developed a localized surface plasmon resonance (LSPR) biosensor made of silver nanoparticles array to detect the cervical cancer using the squamous cell carcinoma antigen (SCCa), as a tumor biomarker. The LSPR helps in overcoming disadvantages and provides good sensitivity and selectivity. The anti-SCCa antibodies were functionalized using 11-mercaptoundecanoic acid. The biosensors were incubated in different concentrations of standard SCCa solution and LSPR values increased stepwise with increasing SCCa concentrations. Thus, the custom-built LSPR system is available for quantitative analysis of SCCa level in human serum with advantages in terms of a rapid test time, label-free, and dilution-free process [25].

In another study, a label-free surface plasmon resonance cytosensor for breast cancer cell detection was produced by the nano-conjugation of monodisperse magneticnanoparticle and folic acid. The biosensor was based on surface surface plasmon resonance (SPR) spectroscopy and had a magnetic nanoparticle combined with MUC1 aptamer and folic acid. The detection ability of this nanosystem was as low as 500 MCF-7 breast cancer cells  $\text{mL}^{-1}$ . It was concluded that the MUC1 aptamer and folic acid improved the sensitivity and selectivity of SPR biosensors [26].

Chen et al developed a generic nanosensor for targeting-free cancer cell screening. The visual screening of cancer cells from normal cells was done by glucose sensitivity of the cancer cells. The Ag/Au nanoshells were glucose oxidase-modified to act as a plasmonic diagnostic tool. The nanosensors were capable of distinguishing the malignant human cervical cancer cell line (HeLa) and the nonmalignant mouse embryonic fibroblast cell line (L929). The cells were found to adhere to the nanosensor with an increase in the period of incubation [27].

## 2.2 *In vivo* investigations of nanocomposites based cancer diagnosis

The *in vivo* research, mainly focuses on the better understanding of overall effects of the developed nanocomposite on the living subjects. It usually engages animal testing or clinical trials. The study of nanocomposite based cancer diagnosis in *in vivo* condition is conceded with a mice model. The principle involved in nanocomposite based *in vivo* cancer visualization is diagrammatically represented in figure 3.

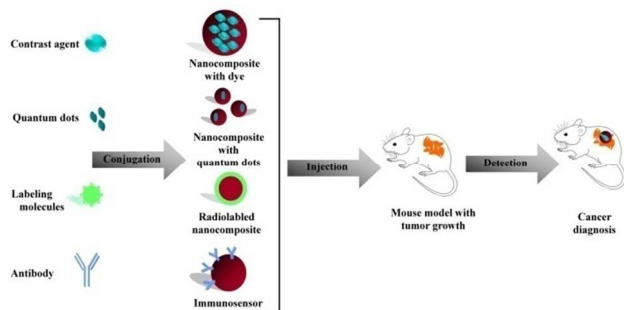


**Figure 3.** Principle involved in nanocomposite based *in vivo* visualization

An *in vivo* evaluation of nanodevices made of porous silicon nanoparticles encapsulated with solid lipid nanoparticles (THCPSi-SLNCs) in the mice model was recorded. The  $^{18}\text{F}$  radiolabeling was incorporated for proper imaging of the breast cancer cells found. Tumor uptake of  $^{18}\text{F}$  loaded THCPSi-SLNCs was found to be higher when compared to the  $^{18}\text{F}$  loaded THCPSi nanoparticles in the subsequent 7 weeks after tumor inoculation. Both the nanodevices were found to be cleared quickly from the circulation and to accumulate in the liver and spleen. Further

material characterization of the nanodevice is needed to promote them [28].

Tian *et al* synthesized nanoamplifiers from gadolinium and gold nanocomposites for magnetic resonance imaging of the colon cancer in both *in vivo* and *in vitro* conditions. Electron transfer between water and gadolinium-doped nanoparticle, which is apparent in the presence of gold, explained the enhancement of signal sensitivity. The tumor-targeted nanoamplifiers were injected into mouse models of colon cancer liver metastasis. It was inferred that the nanoamplifiers enhanced the MRI and optical imaging with considerable contrast improvement despite the gold nanoparticles departure. The amplification was more noticed during the invasive targeted imaging [29].

The various principals involved in the *in vitro* and *in vivo* experimentation of nanocomposite based cancer diagnosis are tabulated in table 1. From the table, nanocomposite based cancer diagnosis includes the gold nanoparticles, TiO<sub>2</sub> nanoparticles, chitosan, CNT and graphene. The TiO<sub>2</sub> nanoparticle possesses redox selectivity, photocatalyst and tunable magnetic property, whereas the chitosan is said to be more biodegradable and biocompatible [10]. The gold nanoparticles have unique optical, electronic and molecular-recognition properties, which makes them promising a nanomaterial [71, 9]. Whilst, the carbon allotropes have their extraordinary strength, thermal conductivity, electrical properties and specifically graphene are transparent helping the nanocomposite to be flexible [73]. It is evident that the carbon allotropes such as CNT and Graphene are equally employed as the gold nanoparticles. Every nanomaterials have their own pros and cons. It is difficult to weigh up a particular nanomaterial to be perfect. Regardless of a nanocomposite's exclusive properties, they may yield different ability depending upon the application. Hence, it becomes more complicated to find a versatile nanocomposite by comparing their property for all applications. The various characteristics of cancer such as stages, type, site it develops varies from person to person, making it more difficult to find a particular nanocomposite as best.

It is also inferred that more concentration is given to the precise properties of a cancer cell than an improvement to conventional visualization techniques leading to the development of immunosensors and nanoaptamers. As there are more trails have been conducted using clinical samples with these nanocomposites, it is high time that steps are taken to introduce these types of diagnosis in human trials. The experimentation of nanocomposite with contrast agent and radiolabbling has been, presently initiated in *in vivo* condition. In depth studies regarding the effects of these immunosensors, contrast agents, radiolables in normal renal cells and other allergic reactions must be studied. These examinations may be carried out in diverse animal models promoting the personalized diagnosis of cancer.

Table 1: Nanocomposites and its principles involved in cancer diagnosis

Nanocomposite	Principle involved	Reference
<i>In vitro</i>		

Poly (methyl methacrylate), single walled carbon nanotube, polyglycolic acid encapsulation	The choline derivate - and gadolinium - based contrast agents enhanced the MRI visualization.	[14]
Gold nanoparticle & chitosan	The electron-transfer resistance was measured with different concentration of K562 leukemia cells	[15]
Chitosan , cadmium-telluride & quantum dots	Amine terminated probe DNA was conjugated for detection of chronic myelogenous leukemia (CML)	[16]
Titanium isopropoxide and mutiwalled carbon nanotube	Electrochemical studies was conducted in K562 cells with nanocomposite.	[17]
Gold nanoparticles, polystyrene (PS) & polyaniline (PANI) core-shell nanocomposite	Measurement of the electron transfer resistance in the HL-60 leukemia cells with nanocomposite suspension	[18]
Copper monosulfide nanoparticle & graphene oxide	Levels of extracellular H <sub>2</sub> O <sub>2</sub> were detected from the HeLa cell culture	[19]
Porous graphine oxide/ Au composites & polytetrafluoroethylene alloy	The mucin protein 1, tumor marker showed amplification and selectivity of MCF-7 cells	[20]
Gold nanoparticle , [9,9-bis(6'-N,N,N-trimethylammonium)hexyl)fluorenyldivinylene-alt -4,7-(2,1,3,- benzothiadiazole) dibromide] (PFVBT) polymer, folate	The folate enhanced the selectivity while gold nanoparticle helped in maintain the fluorescence	[21]
Carbon nanotube, Chitosan & Graphite	The electrodes contained the lung cancer biomarkers such as anti-MAGE A2 and anti-MAGE A11	[22]
Au nanoparticles & TiO <sub>2</sub> nanoparticles	Glucose oxidase (GOD) and ferrocene labelled secondary antibodies (Fc-Ab2) were used to provide amplified signals.	[23]
Silica coated superparamagnetic nanoparticle & N-(2-aminoethyl)-3-aminopropyltrimethoxysilane containing quantum dots	The conjugated anti-CEA antibodies recognized the antigens in the SPCA-1 cells and emitted fluorescence	[24]
Surface plasmon resonance (LSPR) biosensor made of silver nanoparticles array	The anti-SCCa antibodies were functionalized to the biosensors to help in the quantitative analysis of cancer	[25]
Monodispersed magnetic nanoparticles	Magnetic nanoparticle combined with MUC1 aptamer and folic acid to improve the selectivity	[26]
Glucose oxidase-modified Ag/Au nanoshells	Glucose responsive ability of the cancer cells were used for detection	[27]
<i>In vivo</i>		
Porous silicon nanoparticles & solid lipid nanoparticles	<sup>18</sup> F radiolabeling was incorporated for imaging of the breast cancer cells in mice model	[28]
Gadolinium & gold nanoparticles	The electron transfer between water and gadolinium-doped nanoparticle enhanced the MRI images.	[29]

### 3. Nanotechnology in cancer therapy

Cancer treatment differs based on the type, location and stage of the cancer. The choice of treatment includes chemotherapy, radiotherapy, surgery and advanced targeted therapies [30]. The nanotechnology plays a main role in the targeted drug delivery of

anticancer drugs. These nanocarriers have enhanced permeability and preferentially append to the cancer cells. The drugs loaded are usually released through a pre-defined mechanism [31]. Yet another principle involved in the nanotechnology based cancer therapy is photodynamic therapy. In this case, the nanoparticles with light sensitive molecules are irradiated by light become toxic to the malignant cells [32].

### 3.1 *In vitro* investigations of nanocomposites based cancer therapy

Experiments performed in *in vitro* conditions are made using cells or other biological molecules outside the biological context. This type of experimentation reduces the complexity and helps in finding the interaction with the individual components of our interest. The nanocomposite based *in vitro* investigations include targeted drug delivery and combinational photodynamic therapy, which are discussed further. The pictorial representation of the principle involved in nanocomposite based cancer therapeutics is given in figure 4.

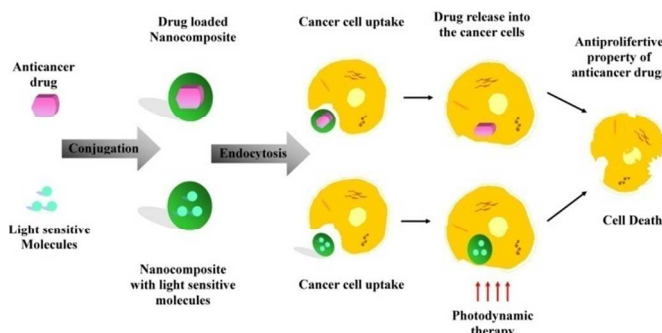


**Figure 4.** Principle involved in nanocomposite based cancer therapeutics

#### 3.1.1 Targeted drug delivery

Targeted drug delivery may also be referred as smart drug delivery as it involves the delivery of medication particularly to the diseased tissue. The drug delivery system is highly integrated and usually made up of a biodegradable material [33]. Meenach *et al* recorded the characterization of poly (ethylene glycol) PEG-iron oxide hydrogel nanocomposites for dual hyperthermia and Paclitaxel delivery to the A549 lung adenocarcinoma cells in *in vitro* condition. The nanosystem comprises of PEG methyl ether methacrylate ( $n=1000$ ) and PEG dimethacrylate with iron oxide entrapped within hydrogel matrices. The hydrogel nanocomposite was heated by an alternating magnetic field. The regions with lower swelling ratios of hydrogel matrices was found to heat to a higher extent. The release of Paclitaxel did not follow the Fick's law of diffusion and the amount of drug release depended on the hydrogel network structure. The cells were exposed in different time periods 3h, 1 day as well as 3 days. There was a decrease of the viable cells after with an increase in the duration of exposure. The efficiency was found to improve in combination of the heat treatment [34]. The layered nanocomposite gallery of  $\text{Na}^+$  Montmorillonite ( $\text{Na}^+$ -MMT) with chitosan was used to deliver the effectual chemotherapeutic drug 5-Fluorouracil (5-FU) for A549 human lung adenocarcinoma epithelial cell line in *in vitro* condition. The MMT and chitosen were at a ratio of 4:1. The drug release from the layered nanocomposite followed

the Fickian diffusion mechanism. The cell viability tests showed  $\text{IC}_{50}$  values of 5-FU, 5-FU-MMT hybrid and 5-FU/CS-MMT composites in A549 cell line were 10.38  $\mu\text{g/ml}$ , 0.34  $\mu\text{g/ml}$  and 11.49  $\mu\text{g/ml}$  was obtained. These results showed that the antitumor effectiveness of 5-FU was preserved even after intercalation of biopolymer in clay. The drug-loaded hybrid composite caused 35% of DNA damage after 3h treatment, which gradually increased to 75 % at 10 h treatment [35].

The synthesis, characterization and *in vitro* studies Doxorubicin-loaded magnetic nanocomposites was done. The co-polymer prepared from N-isopropylacrylamide (NIPAAm) and methacrylic acid (MAA) via radical polymerization was loaded with Doxorubicin. As the N-isopropylacrylamide (NIPAAm) and methacrylic acid (MAA) polymers are temperature sensitive, the release of doxorubicin was influenced by temperature changes. About 0.05% of doxorubicin was released at 37°C and 2.5% of doxorubicin was released at 40°C, with 40 mins of exposure. The Doxorubicin-loaded PNIPAAm-MAA-grafted magnetic nanoparticles had time-dependent effect on the A549 lung cancer cells. The  $\text{IC}_{50}$  of Doxorubicin-loaded PNIPAAm-MAA-grafted magnetic nanoparticles was found to be 0.16 to 0.20 mg/ml [36]. A recent study on the controlled release of Doxorubicin from electrospun PEO/chitosan/graphene oxide nanocomposite (PEO/CS/GO) nanofibrous for the treatment of A549 cells in *in vitro* conditions. The release rate of Doxorubicin from PEO/CS/GO/Doxorubicin nanofibrous was very slow in both neutral and acidic conditions compared with GO/ Doxorubicin. It was found that the hydrophobic force including  $\pi$ - $\pi$  stacking, hydrogen bonding, electrostatic interaction between GO and Doxorubicin and diffusion of Doxorubicin from pores of nanofibers were responsible for slower release of Doxorubicin from PEO/CS/GO/ Doxorubicin nanofibrous. After 72 h treatment of the cell growth was inhibited. The Doxorubicin-loaded PEO/CS/ GO nanofibers exhibited obvious cytotoxicity against A549 cells for longer time than free DOX due to its slower release. This promoted the electrospun PEO/CS/GO/ Doxorubicin nanofibrous in lung cancer treatment [37].

A smart multifunctional nanocomposite that encompasses the magnetic induced target delivery, cell uptake promotion and controlled drug release in one system was developed and experimented with MCF-7 breast cancer cells. The amino-modified mesoporous nanocomposite with Folate conjugation was loaded with Doxorubicin in the mesopores, which had acid sensitive blockers in its orifices. This set up enhanced the pH-dependent self-release. Along with this Folate was also introduced to improve the targeted delivery of Doxorubicin. The release of the Doxorubicin happened in the acidic pH level. There was 80% uptake of Doxorubicin by the MCF-7 through endocytosis at 5 h. Along with this, there was also nuclear fragmentation and condensation in the MCF-7 cells [38]. Biodegradable nanocomposite fibers based on Poly(2-hydroxy ethyl methacrylate) and bamboo cellulose was developed to deliver Paclitaxel to the MCF-7 cancer cells. The prepared nanocomposite fibers showed 96% cell viability while the Paclitaxel incorporated pHEMA-bamboo cellulose nanocomposite fiber showed 7.4% cancer cell viability after 72 h incubation. This confirms the biocompatibility as well as the anticancer effect of Paclitaxel after the incorporation to the pHEMA nanocomposites [39].

Ali *et al* prepared a hippuric acid zinc layered hydroxide nanocomposite (HAN) for delivery of Doxorubicin and Oxaliplatin in the MDA-MB231, MCF-7 cancer cell lines. The hippuric acid zinc layered hydroxide nanocomposite was prepared by the direct reaction of a HA solution with an aqueous suspension of ZnO. The

hippuric acid zinc layered hydroxide nanocomposite with the anticancer drugs was found to inhibit the cell growth of both the cell lines in comparison to the drugs alone. The  $IC_{50}$  value for the combination of HAN with Doxorubicin toward MCF-7 was  $0.19 \pm 0.15 \mu\text{g/mL}$  and toward MDA-MB231 was  $0.13 \pm 0.10 \mu\text{g/mL}$ . The combination of HAN ( $0.5 \mu\text{g/mL}$ ) with Doxorubicin ( $0.5 \mu\text{g/mL}$ ) reduced the cell proliferation in MCF-7 and MDA-MB-231 cells in 37.3% and 17.6%, respectively after 24 hours treatment [40].

This was followed by preparation of iron oxide magnetic nanoparticles coated with chitosan to form CS-MNP nanoparticles. The CS-MNP were loaded with an anticancer drug, betulinic acid (BA) to form a BA-CS-MNP nanocomposite. The release of the BA from the nanocomposite happened at pH 7.4 followed a pseudo-second-order kinetic model. The potential cytotoxicity of free BA, MNPs, CS-MNP, and the BA-CS-MNP nanocomposite was examined in normal mouse fibroblast cells (3T3) and breast cancer cells (MCF-7). No changes were observed due to BA and the nanocomposite at concentrations in the range  $0.781\text{--}50 \mu\text{g mL}^{-1}$  after 72 h of incubation. The BA and BA-CS-MNP nanocomposite exhibited cytotoxicity in MCF-7 cells in a dose-dependent manner with  $IC_{50}$  values of 2 and  $3.6 \mu\text{g mL}^{-1}$ , respectively [41].

A nanocomposite capsule of porous silicon with an acid degradable acetalated dextran (AcDX) matrix was loaded with the Memthotrexate, Paclitaxel and Sorafenib was tested for its therapeutic effect on MCF-7 and MDA-MB-231 breast cancer cell lines. In order to assist the intracellular drug delivery, a nano-arginine cell-penetrating peptide (CPP) was chemically conjugated to the surface of the nanocomposites using oxime click chemistry. The cellular uptake of the nanocomposite was improved by the conjugation of CPP. The release of the anti-cancer drugs was initiated by the pH change to 5.0. Both cell lines had a particle dose-dependent viability towards the bare nanocomposite after 24 h of incubation and a slight decrease of the cell viability was seen with CPP loaded nanocomposite, implying the cell uptake. For both cell lines tested, the combination of Memthotrexate, Paclitaxel and Sorafenib remarkably reduced the cell growth in a concentration-dependent manner. However, at the same concentration range, multidrug loaded nanocomposites showed different effects on the cell proliferation before and after CPP functionalization [42].

Barahue *et al* developed protocatechuic acid-Mg/Al nanocomposite using the ion-exchanged as well as direct coprecipitation. The loading of protocatechuic acid in nanocomposite synthesized using ion exchange and nanocomposite synthesized using direct method was estimated to be about 24.5% and 27.5% (w/w), respectively. After 72 hours incubation of nanocomposites with MCF-7 human breast cancer, the growth of these cancer cells was suppressed, with  $IC_{50}$  of  $35.6 \mu\text{g/mL}$  for protocatechuic acid in nanocomposite synthesized using ion exchange and  $36.0 \mu\text{g/mL}$  for nanocomposite synthesized using direct method for MCF-7 cells. The cytotoxicity of nanocomposite synthesized using ion exchange was greater than that of nanocomposite synthesized using direct method. This result was in parallel with the higher protocatechuic acid in nanocomposite synthesized using ion exchange compared with in nanocomposite synthesized using direct method [43]. A chitosan coated layered clay montmorillonite nanocomposites was prepared to modulate the oral delivery of Paclitaxel in colonic cancer. The Paclitaxel drug was intercalated into the gallery of montmorillonite by ion exchange reaction, which was then coated with the biopolymer chitosan. The nanocomposites demonstrated a controlled release of Paclitaxel and

1:2 fold improvement *in vitro* anticancer activities towards human colon cancer COLO-205 cells in *in vitro* conditions [44]. Venkatesan *et al* developed a chitosan modified hydroxyapatite nanocarriers-mediated celecoxib targeted delivery in colon cancer cells. The cell proliferation, morphology, cytoskeleton, cellular uptake and apoptosis were analysed of colon cancer cells in *in vitro* condition. The results displayed a significant antiproliferation, apoptosis and time-dependent cytoplasmic uptake of celecoxib-loaded Hap-Cht nanoparticles in HCT 15 and HT 29 colon cancer cells. The cells appeared to be round in shape and irregular with no striations in actin filament organization after 48 h treatment of celecoxib-loaded Hap-Cht nanoparticles. Further, *in vivo* studies were performed [45].

Nanocomposite made of nano  $\text{Fe}_3\text{O}_4$  and polylactide nanofibers loaded with Daunorubicin to cause the induction of cell death of leukemia cancer cells was reported. The number of viable cells decreased when treated with the Daunorubicin loaded nanocomposite. The cellular uptake was demonstrated by the inter-cellular green fluorescence emitted by the Daunorubicin drug. The cell inhibition with the  $9.93 \times 10^{-7}$  and  $1.99 \times 10^{-6}$  mol/L Daunorubicin concentrations in the presence of  $\text{Fe}_3\text{O}_4$  nanoparticles or PLA nanofibers produced no significant difference from that of the cell treated with Daunorubicin alone. However, for Daunorubicin concentrations at  $9.93 \times 10^{-7}$  and  $1.99 \times 10^{-6}$  mol/L, the inhibition rates increased to 31% and 46% for the cell system cultured with Daunorubicin and  $\text{Fe}_3\text{O}_4$ -PLA [46]. Chen *et al* developed a Poly (lactic acid) (PLA) based nanocomposites for targeted drug delivery of Daunorubicin to the leukemia K562 cells. PLA based nanocomposites preparation involved the accumulation of the anticancer drug Daunorubicin on PLA nanofibers combined with  $\text{TiO}_2$  nanoparticles. The observation demonstrated that these new nanocomposites could readily induce the anticancer drug Daunorubicin to accumulate on leukemia K562 cells so that the remarkably enhanced intracellular fluorescence intensity could be observed upon application of the blends of the nano- $\text{TiO}_2$  and PLA nanofibers together with Daunorubicin. This also supported the targeted delivery of Daunorubicin to the leukemia cells [47].

The anti-cancer drug internalization was increased by using the nanocomposite with a combination of gold nanoparticle and multi walled carbon nanotube in the human SMMC-7721 hepatocarcinoma cells. The anticancer drug Daunorubicin was conjugated to the gold-carbon nanotube nanocomposite. There was improvement in the anticancer effect with increase in the concentration of Daunorubicin-loaded nanocomposite when compared to Daunorubicin drug alone [48]. Wu *et al* investigated the anticancer effectiveness of potential pharmacophore agents (o-carborane (Cb), o-carborane-C-carboxylic acid (Cbac1), and o-carborane-C(1)C(2)-dicarboxylic acid (Cbac2) coupling with cadmium telluride quantum dots capped with cysteamine (CA-CdTe QDs) in the SMMC-7721 hepatocellular carcinoma cells. The cell inhibition of SMMC-7721 cancer cells was increased by the CA-CdTe QDs. The  $IC_{50}$  of Cbac1 toward SMMC-7721 cancer cells for 72 hours was about  $344 \mu\text{M}$ . The exhibited cytotoxicity was in relation to the ROS generation and genomic damage via apoptosis pathway. This was attributed to the self-assembly nanocomposites of the carborane-carboxylic acids with CA-CdTe QDs [49]. Swet *et al* evaluated a silica-calcium-phosphate nanocomposite (SCPC75) drug delivery system as a means to localize Cisplatin treatment within the tumor, while reducing systemic toxicity, in a rat model of hepatocellular carcinoma. The SCPC75 nanocomposite was made up of 32.9%  $\text{SiO}_2$ , 11.4%  $\text{P}_2\text{O}_5$ ,



22.8% CaO, and 32.9% Na<sub>2</sub>O composition in molar percentage. After this the Cisplatin drug was loaded to the nanocomposite. The Cisplatin was bound to the SCPC75 at  $14.2 \pm 0.2$  mg Cisplatin/g SCPC75. The nanocomposite reduced the cell viability of H4IIE hepatoma cells grown in the culture with time dependency. The experiment was extended and the Cisplatin drug delivery by SCPC75 nanocomposite was conducted in ACI rats [50].

A nanosystem with gold nanorods (AuNRs) encapsulated in nanographene oxide shells was developed to improve the efficiency of chemophotothermal cancer therapy of hepatoma Huh-7 cells. The hyaluronic acid was conjugated in the corners of nanographene oxide wrapped AuNR nanocomposite (NGOHA-AuNRs). The anticancer drug Doxorubicin was loaded to exhibit pH sensitive release. At *in vitro* experiment condition, there was release of 15.9% Doxorubicin at pH 5.3. The cellular uptake of nanocomposite loaded with Doxorubicin was said to be enhanced by hyaluronic acid. The therapeutic efficacy of NGOHA-AuNRs-Doxorubicin presented significantly synergistic chemophotothermal therapy effects that were about 1.5-fold and 4-fold higher than that of separate chemotherapy and photothermal treatment to targeting the Huh-7 cells [51]. Chandran *et al* developed a nano-drug delivery system based on an electric field and pH dual-stimuli responsive chitosan-gold nanocomposite (CGNC) for site specific controlled delivery of the anticancer drug 5-Fluorouracil. The release of 5-Fluorouracil happened at the pH of 5.3, near the cancer cells. The SiHa cells were found to grow on the CGNC-fluorouracil conjugate modified ITO plate. Further application of an electric field of 1.5 V for the release of 5-FU led to the complete death of the SiHa cells [52].

Another nanocomposite was prepared by radical polymerization of methacrylic acid around carbon nanotubes in the presence of Quercetin as a biologically active molecule. The anticancer activity of the flavonoid quercetin was investigated using the HeLa cervical cancer cells. It was found that the covalent conjugation of Quercetin to the polymeric backbone containing dispersed carbon nanotubes is a key process, increasing its anticancer efficiency by increasing the flavonoid stabilization and the cell internalization. Cell viability tests on healthy cells demonstrated no-toxicity due to the quercetin conjugated nanocomposite [53].

### 3.1.2 Photodynamic therapy

Photodynamic therapy is a treatment that uses a photosensitizer or photosensitizing agent, and a particular type of light. When photosensitizers are exposed to a specific wavelength of light, they produce a form of oxygen that kills nearby cells. The type of light and the photosensitizer utilized usually depends on the type of cancer cells involved. The combination of nanotechnology with photodynamic therapy has been welcomed around the globe [54].

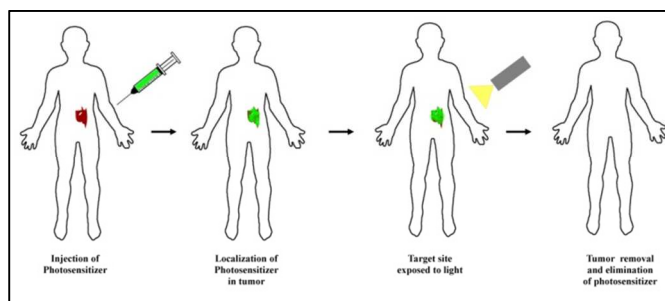


Figure 5: Procedure involved in photodynamic therapy

Xu *et al* used gold-doped TiO<sub>2</sub> (Au/TiO<sub>2</sub>) nanocomposites to improve the photocatalytic inactivation effect on human colon carcinoma LoVo cells. The Au/TiO<sub>2</sub> samples doped with different amounts of Au (1 wt%, 2 wt%, 4 wt%) were prepared by a chemical reduction method and used to photo kill the LoVo cells and it was observed that the most efficient sample was 2 wt% Au/TiO<sub>2</sub>. The study revealed that the irradiation of UV light ( $\lambda_{\text{max}}=365$  nm, intensity=1.8 mW/cm<sup>2</sup>) for 110 min, all of the LoVo cancer cells were killed by 50  $\mu\text{g/mL}$  Au/TiO<sub>2</sub>. The 50  $\mu\text{g/mL}$  TiO<sub>2</sub> nanoparticles killed only 70% cancer under the same condition [55]. The photothermal activity of single walled carbon nanotube (SWCNT) composite with a designed peptide structure of H-(Lys-Phe-Lys-Ala)-7-OH [(KFKA)7] against colon tumor cells was evaluated. The thermographic observations show that intratumoral injection of SWCNT-(KFKA)7 solution followed by NIR irradiation resulted in a rapid increase of the temperature to 43°C in the subcutaneously inoculated colon 26 tumors. There was a remarkable cell damage in the colon 26 culture incubated SWCNT-(KFKA)7 over 3 minutes near infrared irradiation. The single treatment with SWCNT-(KFKA)7 or NIR irradiation did not produce any moderate changes. These results suggest the a great potential of an SWCNT-peptide composite for use in photothermal cancer therapy [56].

Nanocomposite based delivery of anti-cancer agents such as Paclitaxel, 5-Fluorouracil, Doxorubicin, Oxaliplatin, Memthotrexate, Sorafenib, Daunorubicin have been carried out in various cell lines. The significant findings of those investigations are tabulated in the table 2. The majority of the key findings is associated to the cell viability assays. The mode of cell death induced by the targeted delivery of these standard drug merged with nanocomposite should be compared with the mode of cell death induced by these drugs alone. Even though some of the researches explore the anti-proliferative property of phenolic acids, it is most notable that more importance is given to approve anticancer drugs.

**Table 2:** *In vitro* investigation utilizing nanocomposite against various cancer cells

Nanocomposite	Drug delivered	Cell line tested	Key findings	Reference
Poly(ethylene glycol) PEG-iron oxide hydrogel nanocomposites	Paclitaxel	A549 human lung adenocarcinoma cells	> Decrease of the viable cells after with increase in the duration of	[34]

			<ul style="list-style-type: none"> <li>➤ exposure</li> <li>➤ Increase in the efficiency during heat treatment</li> </ul>	
Na <sup>+</sup> Montmorillonite (Na <sup>+</sup> - MMT) with chitosan nanosystem	5-Fluorouracil	A549 human lung adenocarcinoma cells	<ul style="list-style-type: none"> <li>➤ The IC<sub>50</sub> value of 5-FU/CS-MMT composites in A549 cell line were 11.49 µg/ml.</li> <li>➤ The nanodevice caused DNA damage that increased with respect to time</li> </ul>	[35]
N-isopropylacrylamide (nippaam) and methacrylic acid (MAA) grafted nanosystem	Doxorubicin	A549 human lung adenocarcinoma cells	<ul style="list-style-type: none"> <li>➤ Time-dependent effect</li> <li>➤ IC<sub>50</sub> of Doxorubicin-loaded pnippaam-MAA-grafted nanodevice was 0.16 to 0.20 mg/ml</li> </ul>	[36]
PEO/chitosan/graphene oxide nanocomposite	Doxorubicin	A549 human lung adenocarcinoma cells	<ul style="list-style-type: none"> <li>➤ Initiation of cytotoxicity with increased period of exposure</li> </ul>	[37]
Amino-modified Mesoporous nanocomposite with Folate conjugation	Doxorubicin	MCF-7 human breast adenocarcinoma cell line	<ul style="list-style-type: none"> <li>➤ Nuclear fragmentation and condensation in the MCF-7 cells</li> </ul>	[38]
Poly(2-hydroxy ethyl methacrylate) and bamboo cellulose nanosystem	Paclitaxel	MCF-7 human breast adenocarcinoma cell line	<ul style="list-style-type: none"> <li>➤ 7.4% Breast cancer cell were viable after 72 h treatment</li> </ul>	[39]
Hippuric acid zinc layered hydroxide nanocomposite	Doxorubicin and Oxaliplatin	MDA-MB231 breast cancer cell MCF-7 human breast adenocarcinoma cell line	<ul style="list-style-type: none"> <li>➤ The IC<sub>50</sub> toward MCF-7 was 0.19 ± 0.15 µg/ml and toward MDA-MB231 was 0.13 ± 0.10 µg/ml.</li> <li>➤ Cell proliferation in MCF-7 and MDA-MB-231 cells reduced to 37.3% and 17.6%, respectively after 24 h treatment</li> </ul>	[40]
Iron oxide magnetic nanoparticles coated with chitosan	Betulinic acid	MCF-7 human breast adenocarcinoma cell line	<ul style="list-style-type: none"> <li>➤ Cytotoxicity in MCF-7 cells was dose-dependent</li> <li>➤ The IC<sub>50</sub> value of 3.6 µg ml<sup>-1</sup></li> </ul>	[41]
Nanocomposite capsule of porous silicon with acetalated dextran (acdx) matrix	Memthotrexate, Paclitaxel and sorafenib	MCF-7 human breast adenocarcinoma cell line MDA-MB-231 breast cancer cell lines	<ul style="list-style-type: none"> <li>➤ Concentration dependent reduction in the cell viability</li> </ul>	[42]
Protocatechuic acid-Mg/Al nanocomposite	Protocatechuic acid	MCF-7 human breast adenocarcinoma cell line	<ul style="list-style-type: none"> <li>➤ Suppression of cell growth in dose dependent manner</li> </ul>	[43]
Chitosan coated layered clay montmorillonite nanocomposites	Paclitaxel	COLA-25 human colon cancer cells	<ul style="list-style-type: none"> <li>➤ Improvement of Paclitaxel anticancer activity</li> </ul>	[44]
Chitosan modified hydroxyapatite nanocarriers	Celecoxib	HCT 15 and HT 29 colon cancer cells	<ul style="list-style-type: none"> <li>➤ Time-dependent cytoplasmic uptake of celecoxib-loaded Hap-Cht nanoparticles</li> <li>➤ round shaped cells with</li> </ul>	[45]

			no striations in actin filaments organization	
Nano Fe <sub>3</sub> O <sub>4</sub> and polylactide nanofibers nanodevice	Doxorubicin	K562 human leukemia cells	➤ Inhibition of cell growth increased to 31% and 46%	[46]
PLA nanofibers combined with tio <sub>2</sub> nanoparticles	Daunorubicin	K562 human leukemia cells	➤ Accumulation of anticancer drug to leukemia K562 cells	[47]
Gold nanoparticle and multi walled carbon nanotube	Daunorubicin	SMMC-7721 human hepato carcinoma cells	➤ Anticancer effect with increase in the concentration of daunorubin-loaded nanocomposite	[48]
Cadmium telluride quantum dots capped with cysteamine (CA-cdte qds)	O-carborane-C-carboxylic acid	SMMC-7721 human hepato carcinoma cells	➤ The IC <sub>50</sub> was about 344 μm. ➤ Cytotoxicity was in relation to the ROS generation and genomic damage via apoptosis pathway	[49]
Silica-calcium-phosphate nanocomposite (SCPC75) drug delivery system	Cisplatin	H4IIE rat hepatome cells	➤ Time dependent reduction in cell viability	[50]
Gold nanorods (aunrs) encapsulated in nanogrphenoxide shells with hyaluronic acid Conjugation	Doxorubicin	Huh-7 hepatoma cells	➤ Enhanced chemophothermal therapy effects than that of separate chemotherapy and photothermal treatment	[51]
Chitosan-gold nanocomposite (CGNC)	5-Fluorouracil	SiHa cervical squamous carcinoma cells	➤ Complete death of the siha cells when 1.5 V electric field is passed	[52]
Methacrylic acid carbon nanotubes devices	Quercetin	HeLa cervical cancer cells	➤ Increasing its anticancer efficiency by increasing the flavonoid stabilization and the cell internalization	[53]
gold-doped tio <sub>2</sub> (Au/tio <sub>2</sub> ) nanocomposites	-	Human colon carcinoma lovo cells	➤ Improve the photocatalytic inactivation effect on human colon carcinoma lovo cells. T ➤ At UV irradiation, all the lovo cancer cells were killed by 50 μg/ml 2 wt% Au/tio <sub>2</sub>	[54]
Single walled carbon nanotube (SWCNT) c with a designed peptide structure of H-(-Lys-Phe-Lys-Ala)-7-OH [(KFKA) <sub>7</sub> nanosystem	-	Colon 26 colon cancer cells	➤ The photothermal effect caused remarkable cell damage after 3 minutes near infrared irradiation	[55]

### 3.2 *In vivo* investigations of nanocomposites based cancer therapy

The *in vivo* investigation may also termed as pre-clinical procedure and is an important procedure in cancer therapy as it initiates the testing of clinical trials. The figure 6 gives a diagrammatic representation of the principle involved in *in vivo* cancer therapy.

Hossain *et al* developed a Doxorubicin/Carbonate apatite nanocomposite that retarded the growth of established colon tumor cells in the BALB/cA nude mice. The delivery of Doxorubicin was enhanced by the pH sensitive carbonate apatite in the nanocarrier. The nanocomposites had high cytotoxicity than that the cytotoxicity of the free Doxorubicin drug alone and also inhibited the tumor growth [57]. Maksimenko *et al* reported the proof of the self-assembly of conjugated with squalene (SQ-gem) together with isocombretastatin A-4 (isoCA-4), a new isomer of the antivascular combretastatin A-4 (CA-4) in the human colon carcinoma xenograft nude mice model. It was found that SQ-gem/isoCA-4 distributed intracellularly as intact nanoparticles whereas the SQ-gem nanoparticles remained localized onto the cell membrane by confocal microscopic observations. The SQ-gem/isoCA-4 nanocomposites induced complete tumor regression up to 93% in the mouse model [58].

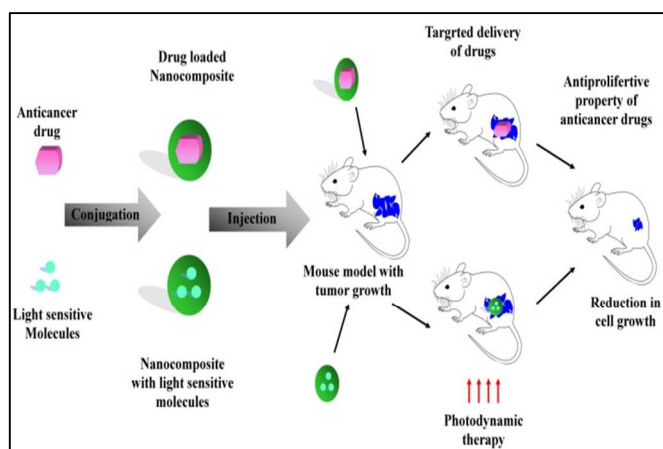


**Figure 6.** Principle involved in nanocomposite based *in vivo* cancer therapy

Venkatesan *et al* proceeded with the *in vivo* investigation after the optimistic results obtained in the *ex vivo* condition as previously stated. The antiproliferative, apoptotic and tumor inhibitory efficacy of celecoxib-loaded nanocomposite in a nude mouse human xenograft model was investigated. *In vivo* human colon tumor xenograft nude mouse tumor studies proved that the celecoxib-loaded Hap- Cht nanoparticles were more potent in inhibiting tumor growth with no prominent side effects. A progressive increase in green fluorescent of the apoptotic cells were found using TUNEL staining in the celecoxib-loaded Hap-Cht nanoparticle-treated group. Based on these results, it is concluded that the Hap-Cht nanocomposite can be an effective and safe vehicle for celecoxib delivery in colon cancer chemotherapy [45].

The drug, the anticancer drug 6-{{2-(dimethylamino)ethyl}amino}-3-hydroxyl-7H-indeno[2,1-c]quinolin-7-one dihydrochloride (TAS-103) was loaded in Poly (lactide-co-glycolide) (PLGA) nanocomposite particles that were inhalable. The drug release of 5%

**Table 3:** *In vivo* investigation utilizing nanocomposite against various mice models

Nanocomposite	Drug delivered	Cell line tested	Key findings	Reference
Doxorubicin/Carbonate Apatite Nanocomposite	Doxorubicin	Colon tumor cells in the BALB/ca nude mice	<ul style="list-style-type: none"> <li>➤ High cytotoxicity than the cytotoxicity of the free Doxorubicin drug alone</li> <li>➤ Inhibition of the tumor</li> </ul>	[57]

TAS-103-loaded PLGA nanocomposite particles signified sustained-release while 10% TAS-103-loaded samples indicated initial burst. The cytotoxicity of A549 was increased by nanocomposites. The cells uptake of nanocomposite followed the endocytosis mechanism. The biodistribution of TAS-loaded PLGA nanocomposite was examined, which showed that there was higher concentration of the drug in plasma in comparison to the intravenous administration of free drug [59].

As previously mentioned, the SCPC75 nanocomposite based delivery of Cisplatin was carried out in *in vivo* condition. Subcutaneous inoculation of H4IIE hepatoma cells caused the reproducible focal tumor mass formation in ACI rats. There was significantly lower tumor growth in the rats treated with SCPC75-Cisplatin hybrid discs than the control and systemic Cisplatin treated. Apart from this the side effects such as rapid weight loss and decreased liver and kidney function induced by systemic Cisplatin was not observed in SCPC75-Cis-treated animals. This shows that the SCPC75 nanocomposite based Cisplatin delivery to be a promising therapy for hepatoma[50].

A synergistic therapy tool that based on CuS nanoparticles-decorated graphene oxide functionalized with polyethylene glycol (PEG-GO/CuS) for cervical cancer treatment. The anticancer drug Doxorubicin was loaded to the PEG-GO/CuS nanocomposites with a the drug loading content as 900 mg Doxorubicin mg<sup>-1</sup>. At acidity of pH 5.5, Doxorubicin was quickly released in the early stage, and about 45% of Doxorubicin was released in the 45 h. There was 75% cell death of the HeLa cells after irradiation at NIR laser at an equivalent of 10 mg/mL Doxorubicin. In mouse models, mouse cervical tumor growth was found to be significantly inhibited by the chemo-photothermal effect of PEG-GO/CuS/Dox nanocomposites, resulting in effective tumor reduction. This demonstrated both the *in vivo* and *in vitro* efficacy of the nanocomposite [60].

A nano-drug delivery system was experimented and in *in vivo* condition and the results were reported. This drug delivery system consists of human serum albumin, poly (lactic-co-glycolic acid) (PLGA), 5-Fluorouracil (5-Fu), magnetic nanoparticles and fluorescent labeling molecule (diphenylhexatriene). The prepared nanocomposite system was tested in the mice model with injected SCC cells. The tumor size was much reduced when injected with nanocomposite containing magnetic nanoparticles than the nanocomposite alone. This was confirmed by visual evaluation as well as the histological analysis [61].

The notable findings recorded during the investigation of nano-drug delivery in *in vivo* condition are given in table 3. It is evident that all these pre-clinical experiments have been carried out with the common anticancer drugs. The nanocomposite based photodynamic therapy has to be initiated in animal models in order to promote their usage in real cancer therapy. This might also help in revealing the other adverse effects in the normal surrounding cells due to this treatment. The evaluation of biodistribution of these nanocomposites in animal model is also necessary to encourage them in clinical cancer treatment.

Squalene gem nanoparticle	Isocombretastatin A-4 (isoca-4)	Human colon carcinoma xenograft nude mice model	growth ➤ Complete tumor regression upto 93%	[58]
Chitosan modified hydroxyapatite nanocarriers	Celecoxib	Mouse human colon cancer xenograft model	➤ Significant antiproliferation, ➤ Apoptosis ➤ Suppression of tumor growth	[45]
Inhalable Poly (lactide-co-glycolide) nanocomposite	6-{{2-(dimethylamino)ethyl}amino}-3-hydroxyl-7H-indeno(2,1-c)quinolin-7-one dihydrochloride (TAS-103)	A549 human lung adenocarcinoma cells injected in mice model	➤ Cytotoxicity of A549 was increased ➤ Higher concentration of the drug in plasma in comparison to the intravenous administration of free drug	[59]
Silica-calcium-phosphate nanocomposite (SCPC75) drug delivery system	Cisplatin	Rat model of hepatocellular carcinoma	➤ Significantly lower tumor growth in the rats treated with SCPC75-Cisplatin hybrid discs than the control and systemic Cisplatin treated	[50]
Cus nanoparticles-graphene oxide with polyethylene glycol (PEG-GO/cus)	Doxorubicin	Mouse model with HeLa cervical cancer cells	➤ 75% cell death of the hela cells after irradiation at NIR laser	[60]
Human serum albumin, poly(lactic-co-glycolic acid) (PLGA) magnetic nanoparticles with diphenylhexatriene	5-Fluorouracil	Mice model with injected SCC cells	➤ Reduction of tumor size inferred from visual and histological analysis	[61]

From the tables 2 and 3, the nanocomposites used for drug delivery utilize PEG, chitosan, NIPAAM, clay montmorillonite, PLA, TiO<sub>2</sub> nanoparticles and gold nanoparticles. Here, the montmorillonite is translucent and has a good thermal stability. Chitosan and PEG are said to have an excellent biodegradability and widely available [11, 75]. The metallic nanoparticles TiO<sub>2</sub> and Gold are said to have an excellent electrical, magnetic and blood compatible [71, 10]. The NIPAAM is more temperature sensitive while PLA is a biodegradable thermoplastic aliphatic polyester [11]. Biodegradability and selectivity are important properties required to develop a potential drug delivering nanosystem. All the nanomaterials are said to exhibit good biocompatibility yet chitosan seems to be a prominent candidate. The superior property of chitosan is that they are biodegradable in acidic pH and are not dissolve in normal physiological pH. Even though they have excellent targeting ability, chitosan nanocomposites cannot be proclaimed as a preferred material for cancer treatment. This is mainly because there is no exhaustive research carried out for a particular nanocomposite/nanomaterial in all types of cancer treatment. This makes difficult to promote a single nanoparticle/nanocomposite as an ideal choice for different cancer treatments.

#### 4. Nanocomposites for simultaneous imaging and drug delivery

The diagnosis and simultaneous drug delivery monitoring through a non-invasive visualization is a challenging task. This is more clinically relevant for killer diseases like cancer. The nanotechnology plays a major role in accomplishing the task. These nanocomposites are frequently called multifunctional nanocomposites and contain both modalities for imaging as well as drugs for treating cancer. Wang *et al* developed a nanocomposite using gold nanoparticle and reduced graphene oxide particles (GNC-RGO) for drug delivery and imaging of the HepG2 cancer cells. The Doxorubicin drug was then loaded to the nanosystem and then exposed to the HepG2 cell culture medium. The Doxorubicin loaded nanosystem effectively transported the drug into the cytoplasm and caused the inhibition of HepG2 cells at high concentration leading to karyopyknosis, shrinkage of the cell nuclei. The GNC-RGO swift absorption by the cells allowed a clear image of the edges and the morphology of the cells, thus showing interesting prospects for cellular imaging while acting as synergistic drug carriers. The Raman spectroscopic investigations showed the presence of GNC-RGO affected the protein  $\alpha$  helices which, if further investigated may depict the mechanism of inhibition of cancer [62].

Another nanodevice made of nanocomposite liposomes containing quantum dots and anticancer drugs for cancer treatment and drug delivery was reported and a comparison of the cationic, PEGylated and deformable liposomes was done. The anticancer drugs camptothecin and irinotecan was encapsulated. The cationic liposomes showed an encapsulation ability of 96% for camptothecin and 99% for irinotecan. Cell viability levels after administration of camptothecin and irinotecan from cationic liposomes at 116  $\mu\text{M}$  were 3.9% and 7.1%, respectively. The cellular uptake of quantum dots from the cationic liposomes was revealed by the red fluorescence emitted from the cytoplasm and near nuclei. In experimentation with the nude mice, once again the cationic liposomes demonstrated the higher tendency to accumulate in solid tumors for exhibiting fluorescence signals compared to other vehicles. Similarly, the intratumoral camptothecin was significant during the administration of cationic liposomes [63].

Seo *et al* prepared a methylene blue-loaded gold nanorod@SiO<sub>2</sub> core (MB-GNR@SiO<sub>2</sub>) are synthesized for use in cancer imaging and photothermal/photodynamic dual therapy. The experiment was carried out in *in vitro* condition using the CT-26 mouse colon cancer cells. The methylene blue molecules were detected at 446, 1380, and 1605  $\text{cm}^{-1}$  in the MB-GNR@SiO<sub>2</sub> nanocomposite. The intensities were poor in case of single cancer cells, while improved due to overlapping of the cancer cells. The cell viability of the cancer cells decreased to 52% when treated with increasing doses of MBGNR@SiO<sub>2</sub> nanocomposites from 0 to 150  $\mu\text{L}$ . The cell viability decreased to 11% for the MB-GNR@SiO<sub>2</sub> cells after NIR laser irradiation for 50 min during photothermal therapy. Along with this, the ROS level was enhanced by the irradiation of the cancer cells [64].

## 5. Conclusion

Revolutionary advances in nanotechnology have transformed the diagnosis and treatment of cancer more advanced. The various features of the nanodevices such as the small size, biocompatibility and ability to penetrate the cells with specificity make them more likely for *in vivo* diagnosis as well as therapy. Some of the benefits and barriers of nanocomposites in cancer are given in figure 7. The involvement of nanodevices allows early diagnosis, better imaging with high specificity, identifying tumor markers, live cell imaging, molecular level examination, understanding the gene mutation and cause of cancer and finally personalization of cancer treatment for individuals.

From our review, it is evident the nanocomposite based cancer diagnosis narrowed to the explicit identification of cancer cells from enhancing of the visualization techniques. Nanocomposites based diagnosis involved the use of conjugated biomarkers [21-24], radiolabeling [25] as well as contrast agents [14] to produce an improved diagnosis. There are also nanosensors to measure the electron transfer resistance and detect the cancer [15-18, 29], which have been experimented in laboratory conditions. As more experimentation of immunosensor and nanoaptamers has already been done with clinical samples, steps to promote them in the medicinal scenario should be initiated. Future improvement of cancer diagnosis to explore the genetic profile of the cancer type

may promote personalized treatment procedures. Chemotherapy is the most commonly adapted treatment procedures for cancer, but the ability to accumulate the drug site-specifically remains subtle. The nano-based drug delivery offers more targeted delivery as well as personalized treatment due to their reduced dimensions and has been gaining momentum in recent years. They reduce the exposure of normal cells to the anticancer drugs. From our study, the approved anticancer drugs such as Doxorubicin [36, 37, 38, 40, 46, 51, 57, 60], Paclitaxel [34, 39, 44], 5-Fluorouracil [35, 52, 61], Daunorubicin [47, 48], Oxaliplatin [40], Cisplatin [50] have been extensively explored.

Some of the chemicals with plant origin are found to have anticancer property and retard the growth of various cancer cells. The nanocomposite-based delivery of these biochemical is to be deciphered to elicit new potential methods for treating cancer. Experimentation of developed nanocomposites for cancer diagnosis and treatment have been conducted in both *in vitro* and *in vivo* conditions along with very few experimentation with the clinical samples. Further, in depth studies in relation to the mode of cell death induced by these drug-delivery systems on cancer cells should be done. The progression of cancer is mediated by distribution of tumor cells through blood system or lymphatic system. These cells that move in the vessels are termed as circulating tumor cells (CTCs) and become the forerunner of metastasis. The count of CTCs are only in the range of  $10^{-7}$  to  $10^{-3}$  among normal blood cells, making them rare and difficult to detect [65]. At present, CTC detectors are based on a mechanical cell-sorting device. Advanced nano-oriented approaches such as, a novel nanotheranostics platform to detect these CTCs to achieve a breakthrough for early detection and treatment cancer should be promoted [66]. Nanotheranostics is an integrated target specific diagnostics and therapeutic tool presented in nano-scale. A smart technique aims to monitor the effect of the therapy given, increasing the drug efficacy and ensuring safety of the patient [67]. Extensive research on various nanotheranostics tools for cancer would help in personalizing the cancer therapy. This may not only help in assessing cancer before or after treatment but also throughout the entire course of therapy.

The overview shows that nanocomposite fabrication employs biomaterials like Poly (methyl methacrylate), polytetrafluoroethylene alloy, Chitosan, Poly (ethylene glycol) PEG that exerts good biocompatibility. It is apparent that chitosan, the biopolymer is utilized predominantly in developing the various nanocomposite for cancer diagnosis and therapy. This may be related to the chitosan's property to have a positive charge under acidic condition allowing the drug delivery and biodegradability [68]. The photodynamic therapy of the nanocomposites is the other area, which needs more attention, particularly in depth *in vivo* experimentation. This investigation would help in recording of the other adverse effect caused to the normal cells surrounding the cancer growth. The effect of the nanocomposite based cancer treatment in knockout mouse (genetically engineered mouse) may obtain efficient information than the *in vivo* studies carried out in mouse models.

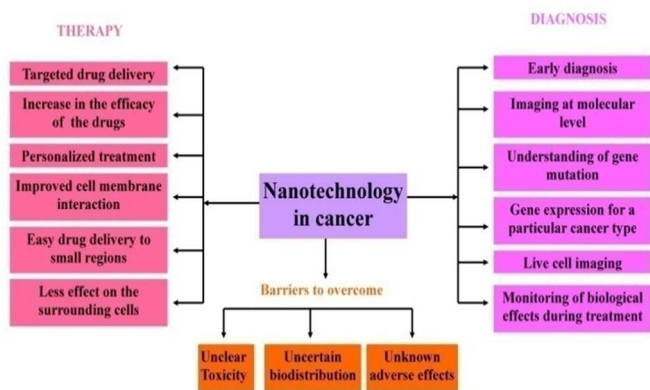


**Figure 7.** Benefits and barriers of nanotechnology in cancer

Apart from these, the toxicity, biodistribution and other adverse effect needs to be recorded carefully. The use of nano-based diagnosis and treatment are increasing especially in cancer. The researchers have been more concentrating to reduce the toxicity of the chemotherapeutic drugs while not realizing the nanodevices may impose risk to the individuals. biocompatibility, solubility and modifying the cellular interaction pathways. Even though the targeted localization of cancer is the key of nanocomposite based diagnosis and treatment, there is still a need for classification of the possible adverse effect on human health. Available literatures with pre-clinical testing suggest that these nanocomposites have an adverse potential. Apart from these, the genotoxicity of the nanocomposites remains to be imperfect [69]. Likewise, there should be a detailed study on the biodistribution of the developed nanocomposite before implementation of the nanoparticles in nanooncology.

In some cases, these nanodevices reach the different body parts via blood stream and pass through the biological protections and accumulate in the some organs and tissue as they are non-degradable. Their common sites of accumulation are lung, bone marrow, liver, kidney, brain and heart [70]. Hence, toxicity of nanocomposites has to be tackled efficiently. More attention on the toxic effect of nanomaterials used in order to prepare the nanocomposite should be done. For example, gold nanoparticles, PEG, CNT are some of the materials that have received significant attention in biomedicine because their unique physical, chemical and biological properties. Despite the potential characteristics, they also exhibit some harmful assets due to long-term administration. Toxicological studies on gold nanoparticle showed their ability to penetrate the red blood cells and cause the sperms to become non-motile [71, 72]. While, some investigation show that CNTs may accidentally penetrate the membrane and damage the dorsal root ganglion neurons [73]. An *in vivo* toxic test revealed that the nanoparticles coated with PEG accumulate in liver and spleen causing acute inflammation [74]. In comparison, the natural nanoparticles such as chitosan, clay montmorillonite are found to have less toxic effect than these synthetic nanocomposites. These natural substances are abundant in nature as well as biocompatible. Besides, they also tend to reduce the toxicity of synthetic nanomaterial when used in combination. In a particular study, the chitosan reduced the toxicity of gold nanoparticles when used for small hairpin RNA delivery to treat human lung adenocarcinoma cells [75].

Yet another promising strategy to overcome this toxic effect is functionalization. The functionalization of these materials reduces the cytotoxicity by increasing their biocompatibility and biodegradability. In case of CNT, the biocompatibility and low cytotoxicity is influenced by the size, dose, duration, testing systems and surface functionalization. The functionalization may be done covalently or non-covalently using chemicals. The biodegradability of functionalized CNTs remained to be ambiguous. While a latest study proved that, the functionalized CNTs were degradable by oxidative enzymes. It also helps in increasing the solubility, biocompatibility, cellular interaction pathways thereby reducing the cytotoxicity of the CNTs [76, 77]. In the near future, synergistic combination of various professionals like oncologists, material engineers, physicians and other biologists may advance the cancer nanotheranostics significantly. This in turn would stimulate a breakthrough in nanooncology and make cancer to be an age-old disease.

## Notes and references

<sup>a</sup> IJN-UTM Cardiovascular Engineering Centre, Faculty of Biosciences and Medical Engineering, Universiti Teknologi Malaysia, Johor Bahru 81310, Malaysia

\*Corresponding author

Dr Saravana Kumar Jaganathan, IJN-UTM Cardiovascular Engineering Centre, Faculty of Biosciences and Medical Engineering, University Teknologi Malaysia, Johor Bahru 81310, Malaysia :Email: [jaganathaniitkcp@gmail.com](mailto:jaganathaniitkcp@gmail.com); Tel : 00607-5558548; Fax: 07-5558553

1. R. Saini, S. Saini, S. Sharma. *Journal of Cutaneous and Aesthetic Surgery* 2010; 3 (1): 32–33.
2. R.R.H Coombs, D.W Robinson. *Nanotechnology in Medicine and the Biosciences*, 3 Vol: Taylor and Francis; 1996.
3. S.K Prasad. *Modern Concepts in Nanotechnology*. Discovery Publishing House. 31–32; 2008.
4. American cancer society. *Cancer Facts & Figures 2015*. Revised February 2015. <http://www.cancer.org/research/cancerfactsstatistics/cancerfactsfigures2015/>
5. C.C Earle, J. Deevy. *Cancer survivorship: Monitoring the long term and late effects of treatment*. In: *Patient Surveillance after Cancer Treatment*. Springer. 2013
6. L. Fass. *Molecular Oncology* 2008; 2 (2008): 115–152.
7. R.C Shetty. *Med Hypotheses* 2005;65 (5): 998–999.
8. W. J. M. Hrushesky, J. Grutsch, P. Wood, Y. Xiaoming, E.Y Oh, C. Ansell. *Integr Cancer Ther* 2009;8:387–397.
9. M. Harrup, A. Wertsching, M. Jones. Chapter 4: Preparation and Characterization of Novel Polymer/Silicate Nanocomposites. In: *Functional Condensation Polymers*; Springer-Verlag: Berlin, 2002; 43-53.
10. P. H. Hoet, I. Bruske-Hohlfeld, O. V. Salata. *J. Nanobiotechnol* 2004; 2:1-12.

11. J. Shi, A.R. Votruba, O.C. Farokhzad, R. Langer. *Nano Lett* 2010;10:3223–3230.
12. C. Loo, A. Lin, L. Hirsch, M.H. Lee, J. Barton, N. Halas, J. West, R. Drezek. *Technol Cancer Res Treat* 2004;3 (1): 33–40.
13. G. Zheng, F. Patolsky, Y. Cui, W.U. Wang, C.M. Lieber. *Nat Biotechnol.* 2005; 23 (10): 1294–1301.
14. K.S. Martirosyan, R.J. Stafford, Elliott, S.J. Frank. PMMA/SWCNT nanocomposites for prostate brachytherapy MRI contrast agent markers. Conference proceedings of NIST-Nanotech 2009;2:44-47
15. L. Ding, C. Hao, Y. Xue, H. Ju. *Biomacromolecules*, 2007; 8 (4):1341–1346.
16. A. Sharma, C. M. Pandey, G. Sumana, U.Soni, S. Sapra, A.K. Srivastava, T. Chatterjee, B.D. Malhotra. *Biosensors and Bioelectronics* 2012;38(2012):107–113.
17. Q. Shen, S.K. You, S.G. Park, H. Jiang, D. Guo, B. Chen, X. Wang. *Electroanalysis* 2008; 20(23): 2526 – 2530.
18. M. Gu, J. Zhang, Y. Li, L. Jiang, J. Zhu. *Talanta* 2009; 80 (2009): 246–249.
19. J. Bai, X. Jiang. *Anal. Chem.* 2013; 85: 8095–8101
20. M. Yan, G. Sun, F. Liu, J. Lu, J. Yu, X. Song. *Anal Chim Acta.* 2013; 798 (2013): 33–39.
21. J. Geng, K. Li, K.Y. Pu, D. Ding, B. Liu. *small* 2012; 8: 15, 2421–2429.
22. M. Choudhary, A. Singh, S. Kaur, K. Arora. *Appl Biochem Biotechnol.* 2014;174(3):1188-1200.
23. Y. Zhuo, Y.Q. Chai, R. Yuan, L. Mao, Y.L. Yuan, J. Han. *Biosensors and Bioelectronics.* 2011; 26 (2011): 3838–3844.
24. J. Ma, Q. Fan, L. Wang, N. Ji, Z. Gu, H. Shen. *Talanta* 2010; 81 (2010): 1162–1169
25. Q. Zhao, R. Duan, J. Yuan, Y. Quan, H. Yang, M. Xi. *Int J Nanomedicine* 2014;9 1097–1104.
26. H. Chen, Y. Houa, Z. Ye, H. Wang, K. Koh, Z. Shen, Y. Shue. *Sensor Actuat B-Chem.* 2014; 201 (2014) 433–438.
27. L. Chen, H. Li, H. He, H. Wu, Y. Jin. *Anal. Chem.* 2015, 87, 6868–6874.
28. A.M. Kallinen, M.P. Sarparanta, D. Liu, E.M. Mäkilä, J.J. Salonen, J.T. Hirvonen, H.A. Santos, A.J. Airaksinen. *Mol. Pharmaceutics* 2014; 11: 2876–2886.
29. X. Tian, Y. Shao, H. He, H. Liu, Y. Shen, W. Huang, L. Li. *Nanoscale* 2013; 5: 3322.
30. M.J. Lind. *Medicine.* 2008; 36 (1): 19–23
31. P. Boisseau, B. Loubaton. *C. R. Phys.* 2011; 12 (7): 620.
32. S.S. Wang, J. Chen, L. Keltner, J. Christophersen, F. Zheng, M. Krouse, A. Singhal. *Cancer Journal* 2002;8: (2): 154–63.
33. M. Wang, M. Thanou. *Pharmacol. Res.* 2010; 62:90–99.
34. S.M. Meenach, J.M. Shapiro, J.Z. Hilt, K.W. Anderson. *Journal of Biomaterials Science, Polymer Edition*, 2013; 24( 9): 1112-1126.
35. B.D. Kevadiya, T.A. Patel, D.D. Jhala, R.P. Thumbar, H. Brahmabhatt, M.P. Pandya, S. Rajkumar, P.K. Jena, G.V. Joshi, P.K. Gadhia, C.B. Tripathi, H.B. Bajaj. *European Journal of Pharmaceutics and Biopharmaceutics* 2012; 81 (2012): 91–101.
36. Akbarzadeh A, Samiei M, Sang WJ, Anzaby M, Hanifehpour Y, Nasrabadi HT, Davaran S. *Journal of Nanobiotechnology* 2012; 10:46
37. B. Ardeshirzadeh, N.A. Anaraki, M. Irani, L.R. Rad, S. Shamshiri. *Materials Science and Engineering C* 2015; 48 (2015): 384–390.
38. C. Wang, P. Lv, W. Wei, S. Tao, T. Hu, J. Yang, C. Meng. *Nanotechnology* 2011; 22 (2011): 1-8.
39. S.S. Rao, S.G. Jeyapal, S.J. Rajiv. *Composites: Part B* 2014; 60 (2014): 43–48.
40. S.H. Hussein-Al-Ali, M. Al-Qubaisi, M.Z. Hussein, M. Ismail, S. Bullo. *Drug Des Devel Ther.* 2013; 7: 25–31.
41. S.H. Hussein-Al-Ali, P. Arulselvan, S. Fakurazi, M.Z. Hussein. *J Mater Sci* 2014; (2014) 49:8171–8182.
42. D. Liu, H. Zhang, E. M€akil€a, J. Fan, B. Herranz-Blanco, C.F. Wang, R. Rosa, A.J. Ribeiro, J. Salonen, J. Hirvonen, H.A. Santos. *Biomaterials* 2015; 39 (2015): 249- 259
43. F. Barahuie, M.Z. Hussein, S.H. Hussein-Al-Ali, P. Arulselvan, S. Fakurazi, Z. Zainal. *International Journal of Nanomedicine* 2013;8: 1975–1987.
44. C. Bothiraja, U.H. Thorat, A.P. Pawar, K.S. Shaikh. *Materials Technology.* 2014; 29(B2):B120-B126
45. P. Venkatesan, N. Puvvada, R. Dash, B.N. Prashanth Kumar, D. Sarkar, B. Azab, A. Pathak, S.C. Kundu, P.B. Fisher PB, Mandal M. *Biomaterials.* 2011;32(15):3794-806.
46. G. Lv, F. He, X. Wang, F. Gao, G. Zhang, T. Wang, H. Jiang, C. Wu, D. Guo, X. Li, B. Chen, Z. Gu. *Langmuir* 2008; 24: 2151-2156.
47. C. Chen, G. Lv, C. Pan, M. Song, M. Wu, D. Guo, X. Wang, B. Chen, Z. Gu. *Biomed. Mater.* 2007; 2 (2007): L1–L4.
48. Q. Li, D. Guo, R. Zhang, X. Wang. *J Nanosci Nanotechnol.* 2012;12(3):2192-2198.
49. C. Wu, L. Shi, Q. Li, H. Jiang, M. Selke, H. Yan, X. Wang. *Nanomedicine: Nanotechnology, Biology, and Medicine* 2012; 8 (2012): 860–869
50. J.H. Swet, H.J. Pacheco, D.A. Iannitti, A. El-Ghanam, A.H. McKillop. *Journal of biomedical materials research B: Applied biomaterials* 2014;102B(1):190-202.
51. C. Xu, D. Yang, L. Mei, Q. Li, H. Zhu, T. Wang. *ACS Appl. Mater. Interfaces* 2013; 5: 12911–12920
52. P.R. Chandran, N. Sandhyarani. *RSC Adv* 2014; 4: 44922
53. G. Cirillo, O. Vittorio, S. Hampel, F. Iemma, P. Parchi, M. Cecchini, M. Puoci, N. Picci. *Eur. J. Pharm. Sci.* 2013; 49: 359–365.
54. Z. Huang. *Technol. Cancer Res. treat.* 2005; 4 (3): 283–93.
55. J. Xu, Z.D. Chen, Y. Sun, C.M. Chen, Z.Y. Jiang. *Acta Chimica Sinica* 2008; 66(10):1163-1167.
56. Y. Hashida, H. Tanaka, S. Zhou, S. Kawakami, F. Yamashita, T. Murakami, T. Umeyama, H. Imahori, M. Hashida. *J Control Release.* 2014;173:59-66.
57. S. Hossain, H. Yamamoto, E.H. Chowdhury, X. Wu, H. Hirose, A. Haque, Y. Doki, M. Mori, T. Akaike. *PLoS ONE* 2013; 8(4):
58. A. Maksimenko, M. Alami, F. Zouhiri, J.D. Brion, A. Pruvost, J. Mougín, A. Hamze, T. Boissenot, O. Provot, D. Desmae'le, P. Couvreur. *ACS Nano* 2014; 8(3): 2018–2032.



59. K. Tomoda, T. Ohkoshi, K. Hirota, G.S Sonavane, T. Nakajim, H. Terada, M. Komuro, K. Kitazato, K. Makino. *Colloids and Surfaces B: Biointerfaces* 2009;71: 177–182.
60. J. Bai, Y. Liu, X. Jiang. *Biomaterials* 2014;35 (2014): 5805–5813
61. H. Misak, N. Zacharias, Z. Song, S. Hwang, K.P Man, R. Asmatulu, S.Y Yang. *J. Biotechnol.* 2013;164 (2013): 130–136
62. C. Wang, J. Li, C. Amatore, Y. Chen, H. Jiang, X.M Wang. *Angew Chem Int Ed Engl.* 2011;50(49):11644–11648
63. C.J Wen, C.T Sung, I.A Aljuffali, Y.J Huang, J. You. *Nanotechnology* 2013; 24: 325101.
64. S.H Seo, B.M Kim, A. Joe, H.W Han, X. Chen, Z. Cheng, E.S Jang. *Biomaterials* 2014; 35 (2014): 3309–3318
65. G.P Gupta, J. Massagué. *Cell* 2006; **127** (4): 679–95.
66. J.W. Kim, E. I. Galanzha, D. A. Zaharoff, R. J. Griffin, V. P. Zharov. *Mol. Pharmaceutics* 2013, 10, 813–830
67. L.S Wang, M.C Chuang, and J. A Ho. *Int J Nanomedicine.* 2012, 7: 4679–4695.
68. W.H.D Jong , P.J Borm. *Int J Nanomedicine.* 2008; 3(2): 133–149.
69. A.L Di Virgilio, M. Reigosa, P.M Arnal, F. Lorenzo de Mele., 2010. *J. Hazard.Mater.* 2010; 177: 711–18.
70. J. Zhao, V. Castranova. *J Toxicol Environ Health B Crit Rev* 2011; 14(8): 593–632.
71. B.M Rothen-Rutishauser, S. Schurch, B. Haenni, N. Kapp, P. Gehr, *Environ. Sci. Technol.*2006; 40: 4353–59.
72. V. Wiwanitkit, A. Sereemasapun, R. Rojanathanes. *Fertil. Steril.* 2009; 91: e7–e8.
73. L. Belyanskaya, S. Weigel, C. Hirsch C, *Neurotoxicology.* 2009;30:702–711.
74. W.S. Cho, M. Cho, J. Jeong, M. Choi, H.Y Cho, B.S Han, S.H Kim, H.O Kim, Y.T Lim, B.H Chung. *Toxicol. Appl. Pharmacol.* 2009; 236: 16–24.
75. S.Jeong, S. Y. Choi, J. Park, J.H. Seo, J.Park, K.Cho, S.W.Joo, S. Y Lee. *J. Mater. Chem.*, 2011,**21**, 13853–13859
76. A. Bianco, K. Kostarelos, M. Prato *Chem. Commun.* 2011. 47 10182–8
77. S.Vardharajula, S.Z Ali, P.M Tiwari, E. Eroğlu, K. Vig, V.A Dennis, S.R Singh. *Int. J. Nanomed.* 2012 7 5361–74